# Binding of a Sequence-Specific Single-Stranded DNA-Binding Factor to the Simian Virus 40 Core Origin Inverted Repeat Domain Is Cell Cycle Regulated

ELLEN P. CARMICHAEL,[1] JANET M. ROOME,[1] AND ALAN F. WAHL[2]*

*Department of Cellular and Molecular Biology, Bristol-Myers Squibb Pharmaceutical Research Institute, Wallingford, Connecticut 06492,[1] and Department of Growth Regulators, Bristol-Myers Squibb Pharmaceutical Research Institute, Seattle, Washington 98121[2]*

The inverted repeat domain (IR domain) within the simian virus 40 origin of replication is the site of initial DNA melting prior to the onset of DNA synthesis. The domain had previously been shown to be bound by a cellular factor in response to DNA damage. We demonstrate that two distinct cellular components bind opposite strands of the IR domain. Replication protein A (RPA), previously identified as a single-stranded DNA binding protein required for origin-specific DNA replication in vitro, is shown to have a preference for the pyrimidine-rich strand. A newly described component, IR factor B (IRF-B), specifically recognizes the opposite strand. IRF-B binding activity in nuclear extract varies significantly with cell proliferation and the cell cycle, so that binding of IRF-B to the IR domain is negatively correlated with the onset of DNA synthesis. Loss of IRF-B binding from the nucleus also occurs in response to cellular DNA damage. UV cross-linking indicates that the core binding component of IRF-B is a protein of ca. 34 kDa. We propose that RPA and IRF-B bind opposite strands of the IR domain and together may function in the regulation of origin activation.

Exposure of transformed mammalian cells to DNA-damaging agents, including UV irradiation, can result in the induction of unscheduled DNA replication and the amplification of a variety of genes (46). This can play an important role in the development of drug resistance (36, 41–43, 46, 56) and may also contribute to transformation and tumor progression (56). The molecular mechanisms of gene amplification remain obscure, but they clearly involve the normal DNA replicative machinery of the cell and the loss of the ability to limit replication to once per cell cycle. The cause of this dysfunction may be genetically linked (51) or related to viral transformation (25, 44).

Because of limited information on the human replicon and how origins of replication are controlled in *cis*, viral systems have proven to be most useful to the study of mechanisms of replication and gene amplification (5, 15, 17, 23, 24, 27, 29, 33, 38, 39, 44, 53, 54, 60). Papovaviruses and parvoviruses can be induced to replicate in various cell lines (permissive or nonpermissive) when the cells are treated with a variety of DNA-damaging agents (38, 53, 60). In simian virus 40 (SV40)-infected permissive cells, the viral genome undergoes multiple rounds of replication during a single cell cycle in a process requiring the virally encoded T-antigen and cellular DNA replication components. In contrast, in SV40-transformed semi- or nonpermissive cell lines, the viral DNA is integrated in the host genome and, under host cell cycle control, is copied only once per S-phase. However, exposure of these infected, nonpermissive cells to DNA-damaging agents (such as UV light or *N*-methyl-*N'*-nitro-*N*-nitrosoguanidine [MNNG]) results in productive replication of the viral sequences as well as amplification of flanking regions of the host genome (25, 26). This cellular response to DNA damage is reported to be mediated by the induction of one or more *trans*-acting factors, since the fusion of DNA-damaged cells to untreated SV40-transformed cells activates SV40 amplification in the heterokaryons (5, 33).

Ronai and Weinstein have demonstrated that UV treatment of normal rat fibroblasts induces proteins which bind within the polyomavirus regulatory region and stimulates polyomavirus replication (39, 40). Similarly, Lücke-Huhle et al. (28) reported induction of a factor(s) binding to the SV40 origin imperfect inverted repeat domain (IR domain, as defined by Parsons et al. [35]) (see Fig. 1A) in response to cell exposure to UV radiation and correlated this increase with DNA damage-induced viral DNA replication (28). Furthermore, cytosolic extracts from MNNG-treated SV40-transformed Chinese hamster cells supported SV40 DNA replication in vitro in the presence of exogenous T antigen, whereas replication by extracts from untreated cells was inefficient (4). Treatment of irradiated cells with duplex oligonucleotides corresponding to the SV40 IR domain inhibited DNA amplification, presumably because the duplex oligonucleotides sequestered a DNA damage-activated factor needed for amplification in vivo (28). In addition, a monkey cell factor binding to sequence encompassing the IR domain has been described (52). The origin IR domain is the site of initial DNA melting prior to the onset of viral DNA synthesis (6, 35). Examination of several papovavirus origins of replication (52) as well as herpesvirus origins of replication revealed significant homology to the IR domain sequence (Fig. 1A).

In synchronized SV40 permissive cells, only cell extracts prepared from cells after $G_1$-to-S-phase ($G_1$/S-phase) transition are capable of supporting SV40 DNA synthesis in vitro (37). Similarly, amplification of the dihydrofolate reductase gene induced by methotrexate or amplification of SV40 in response to DNA damage occurs maximally when the cells are treated in early S-phase (21). This cell cycle dependence occurs despite the fact that many of the key DNA replication proteins appear to be constitutively expressed throughout the proliferative cell cycle (10, 30, 32, 37, 55, 59).

---

* Corresponding author.

We describe here the SV40 IR DNA binding activity of two single-stranded DNA binding factors from nuclear extracts and their regulation during cell growth. To begin to examine the role that SV40 IR factors (IRF) may play in scheduled chromosomal DNA replication, we have characterized factor binding as cells progress from quiescence to proliferation and through the proliferative cell cycle. We have analyzed the interaction of synthetic oligonucleotides derived from either strand of the SV40 origin IR domain with extracts from cells treated with DNA-damaging agents, as well as with extracts from cells staged at different points in the cell cycle. Two cellular single-stranded specific DNA binding proteins, capable of preferentially binding to the opposite strands of the IR domain, are described. Replication protein A (RPA), recently characterized as a single-stranded pyrimidine DNA binding protein (20) and known to be required for origin-specific SV40 DNA replication in vitro (16, 57, 58), is shown to have a preference for the pyrimidine-rich strand of the SV40 IR domain. A newly described component, IRF-B, specifically recognizes the complementary strand. IRF-B activity varies significantly with cell proliferation and the cell cycle so that binding of IRF-B to the IR domain is negatively correlated with the onset of DNA synthesis. IRF-B activity is depleted in the nucleus and induced in the cytosol in response to DNA damage. Taken together, these results suggest that RPA and IRF-B bind to opposite strands of the IR domain and that displacement or inactivation of IRF-B may function in the regulation of origin activation during scheduled cellular DNA synthesis and during DNA amplification from the SV40 origin of replication in response to DNA damage.

## MATERIALS AND METHODS

**Materials.** Poly(dA)$_{2000}$ and oligo(dT)$_{20}$ (Pharmacia) were combined at a 20:1 weight ratio at 1 mg/ml and annealed in 50 mM Tris-HCl (pH 7.5)–1 mM EDTA at 70°C and then slowly cooled. Activated calf thymus DNA was prepared as described previously (8). All chemicals were from Sigma (St. Louis, Mo.) unless otherwise noted. $N^2$-(p-n-Butylphenyl)-2'-dGTP (BuPdGTP) was a gift of G. Wright (University of Massachusetts Medical School). RPA monoclonal antibody (p70-9) directed against the 70-kDa subunit was kindly provided by Bruce Stillman (Cold Spring Harbor Laboratory). Antibodies directed against the 32-kDa subunit of RPA were kindly provided by Marc Wold (University of Iowa). Antibodies directed against p53 (clone 421), retinoblastoma protein (clone C36), and T antigen (pAb 419) were obtained from Oncogene Sciences (Manhasset, N.Y.). Heat shock protein 70 monoclonal antibody SPA-820 was obtained from StressGen Biotechnologies Corp. (Victoria, British Columbia, Canada).

**Cell culture.** The HeLa S3 cell line was obtained from the American Type Culture Collection (Rockville, Md.). MANCA, a human Burkitt's lymphoma B-cell line, was obtained from J. M. Roberts (Fred Hutchinson Cancer Research Center). The cell lines were grown as spinner cultures in Dulbecco minimum essential medium and RPMI medium, respectively, supplemented with 10% fetal bovine serum and 100 U of penicillin G sodium, 100 μg of streptomycin sulfate, and 0.25 μg of amphotericin B (as Fungizone) per ml. IMR90, a normal human diploid fetal lung fibroblast cell line (American Type Culture Collection), was maintained in Eagle minimum essential medium supplemented with 10% fetal bovine serum, nonessential amino acids, L-glutamine, and antibiotics. All media and supplements were obtained from GIBCO Laboratories, Grand Island, N.Y., and from Bethesda Research Laboratories, Inc., Gaithersburg, Md. All cell lines were grown in a humidified 37°C incubator with 5% $CO_2$.

**In vivo DNA synthesis.** DNA synthesis in vivo was monitored for each experimental time point or population by plating $2.5 \times 10^4$ IMR 90 cells or $5 \times 10^5$ HeLa or MANCA cells in 500 ml of complete medium into duplicate wells of a 24-well microtiter plate. Cells were pulse-labeled with [methyl-$^3$H]thymidine (20 Ci/mmol; Amersham Corp., Arlington Heights, Ill.) at 0.025 mCi/ml for 1 h at 37°C prior to harvest. Media and cells were removed to a 1.5-ml microcentrifuge tube, and cells were pelleted at 2,000 × g for 3 min. The medium was removed, and the cell pellet was rinsed twice with ice-cold 5% trichloroacetic acid. The pellet was solubilized in 150 ml of 0.25 M NaOH and combined with 1.0 ml of aqueous scintillation cocktail, and radioactivity was counted.

**UV treatment of cells.** For UV irradiation, cells were grown in 150-mm-diameter plates to 70% confluency. Prior to irradiation, medium was removed and the cells were rinsed once with phosphate-buffered saline (PBS; 137 mM NaCl, 4.2 mM KCl, 9.6 mM $Na_2HPO_4$, 1.1 mM $KH_2PO_4$). The monolayer was exposed to 0.8 J of 254-nm UV light per $m^2$ per s for various times to achieve the appropriate fluence. After irradiation, complete medium was added to each dish and further incubated for 1 h prior to cell extraction.

**Cell proliferation: serum deprivation and restimulation.** Confluent IMR90 cells at 21 population doubling passages were serum deprived to bring about quiescence and restimulated to synchronously proliferate as described previously (54). Cells were harvested for nuclear extract preparation at 6, 10, 16, 20, 24, and 30 h after serum stimulation. Protein concentrations were determined by the Bradford method (7). Cellular DNA synthesis at each time point was monitored in parallel microtiter plates by analysis of [$^3$H]thymidine incorporation.

**Cell cycle studies: counterflow centrifugal elutriation.** Exponentially growing MANCA cells were maintained at densities of $2 \times 10^5$ to $5 \times 10^5$/ml, and fresh medium was added 12 h prior to harvest to enhance logarithmic growth. Cultures were concentrated by centrifugation, and $2 \times 10^8$ cells were gently resuspended in 15 ml of elutriation buffer (PBS with 1% calf serum and antibiotic and antimycotic) and passed through a 18-gauge needle to insure monodispersion. Cells were separated into populations of progressively increasing cell size in a centrifuge (Beckman J-6B) equipped with a JE-6B elutriation rotor at 21°C. MANCA cells were loaded at a rotor speed of 1,800 rpm and a flow rate of 13 ml/min, and 100-ml fractions were collected from 15 to 40 ml/min in 3-ml/min increments. To verify cell cycle progression, following elutriation, a portion of each population was analyzed for cell number and volume with a channelizer (Coulter Electronics, Inc. Hialeah, Fla.); another aliquot was stained with propidium iodide solution and analyzed for DNA content by using a fluorescence-activated cell sorter (FACS-IV; Becton-Dickinson Instruments, Mountain View, Calif.). Cellular DNA synthesis analysis was performed as described above for each population.

**Cell staging by metabolic block.** Logarithmically proliferating HeLa cells were synchronized by double thymidine block (49) by using 2 mM thymidine for 18 h, a 10-h release in fresh medium, and then a second 18-h block prior to release. To release them from block, cells were centrifuged at 1,200 rpm for 5 min in a Beckman GPKR centrifuge,

washed with PBS, and resuspended in fresh medium at 37°C for the times indicated prior to extraction.

**Synthetic oligonucleotides.** Oligonucleotides were synthesized with a Milligen Biosearch 8700 DNA synthesizer by standard phosphoramidite chemistry. Purity was assessed by high-performance liquid chromatography and denaturing gel electrophoresis. For the binding assays, oligonucleotides were end labeled by using polynucleotide kinase to a specific activity of ~4 × $10^6$ cpm/pmol. The sequence of syn16 strand 1 (syn16-1) DNA competitor DNA is 5' TCTAGAAA ATTATTAACCTCA 3'.

**Cell extraction.** Nuclear extracts were prepared from HeLa cells grown to a maximum density of 5 × $10^5$/ml in spinner cultures by the method of Dignam et al. (13) with a few modifications. Cells were centrifuged at 4°C for 10 min at 1,800 rpm to concentrate them, and the cell pellet was washed in ice-cold hypotonic buffer A (10 mM N-2-hydroxy-ethylpiperazine-N'-2-ethanesulfonic acid [HEPES], pH 7.9; 10 mM KCl; 1.5 mM $MgCl_2$; 0.2 mM phenylmethylsulfonyl fluoride [PMSF]; 0.5 mM dithiothreitol [DTT]) and immediately recentrifuged. IMR90 cells were trypsinized from plates, the trypsinization was stopped by the addition of complete medium, and the cells were washed by centrifugation at 1,200 × g for 5 min in ice-cold PBS. Cell pellets were resuspended in 5 pellet volumes of hypotonic buffer A, swelled on ice for 20 min, and lysed by 20 strokes of a Dounce homogenizer. Nuclei were pelleted by centrifugation for 15 min at 4,000 rpm. Supernatant from cell lysis was further cleared by centrifugation at 100,000 × g and frozen in liquid nitrogen (cytosol). The nuclear pellet was gently resuspended in an equal volume of nuclear extraction buffer (20 mM HEPES, pH 7.9; 25% glycerol; 1.5 mM $MgCl_2$; 400 mM KCl; 0.2 mM EDTA; 0.2 mM PMSF; 0.5 mM DTT) and incubated at 4°C with continuous, gentle mixing for 30 min. The extracted nuclei were pelleted at 100,000 × g, and the supernatant was removed, dialyzed overnight against 20 mM HEPES (pH 7.9)–20% glycerol–100 mM KCl–0.2 mM EDTA–0.2 mM PMSF–0.5 mM DTT, and then frozen in liquid nitrogen.

**In vitro DNA polymerase and exonuclease assays.** Assays for DNA polymerase α, δ, and ε activities and for DNA polymerase δ- and ε-associated exonuclease activities were as previously described (11). Inhibition with aphidicolin, SJK132-20 (anti-DNA polymerase α) immunoglobulin G (IgG), and BuPdGTP to differentiate the three DNA polymerases was carried out as previously described (19, 55).

**Partial purification of IRF-A and -B.** Initial steps in the purification of human DNA polymerase δ and the associated IR binding factors were by a modified method of Hamatake et al. (19), including chromatography of the S100 fraction over S Sepharose followed by chromatography over Q Sepharose. The S100 fraction was batch adsorbed for 1 h onto 6 ml of S Sepharose Fast Flow (Pharmacia LKB) preequilibrated in buffer A [50 mM potassium phosphate, pH 7.5; 5 mM DTT; 10% glycerol; 1 mM EDTA; and 1 mM ethylene glycol-bis(β-aminoethyl ether)-N,N,N',N'-tetra-acetic acid (EGTA)]. Unbound protein was removed with three 10-ml centrifugation-resuspension washes with buffer A. The resin was poured into a column (1 by 10 cm), washed with 3 column volumes of buffer A, and step eluted with 10 ml of buffer A plus 0.5 M NaCl. The eluant was adjusted, by the addition of dilution buffer (5 mM DTT, 10% glycerol, 1 mM EDTA, and 1 mM EGTA), to the ionic strength of buffer A plus 0.1 M NaCl and applied at 0.5 ml/min to a 5-ml prepacked and preequilibrated (buffer A with 0.1 M NaCl) Q Sepharose Fast Flow (Pharmacia) column (1 by 10 cm). The

resin was washed with 3 column volumes of buffer A plus 0.1 M NaCl and subsequently eluted with an 8-column volume linear gradient with buffer A plus 0.1 M NaCl to buffer A plus 0.4 M NaCl. Fractions of 1 ml were collected and assayed for DNA polymerase α activity on activated calf thymus DNA, for DNA polymerase δ and ε activities on poly(dA)$_{1000-4000}$ oligo(dT)$_{12-18}$ as described previously (11), and for IR domain DNA binding. To further concentrate the DNA polymerase δ-IRF component, active fractions were pooled, adjusted to the ionic strength of buffer A with dilution buffer, and reapplied to 2 ml of S Sepharose Fast Flow preequilibrated in buffer A. The resin was washed with 2 column volumes of buffer A and step eluted into 0.5-ml fractions with buffer A plus 0.5 M NaCl.

Fractions containing DNA polymerase δ from the S Sepharose step elution were pooled, dialyzed against buffer C (20 mM Tris, pH 7.5; 20% glycerol; 5 mM DTT; 4 mM $MgCl_2$; 0.1 mM EDTA), and chromatographed over a 3-ml column of 5' AMP-Sepharose 4B (Pharmacia) as previously described (11). Fractions containing DNA polymerase δ activity, nuclease activity, and IRF-A activity were dialyzed in buffer containing 20 mM HEPES (pH 7.8), 1 mM DTT, 150 mM KCl, 2.5% (wt/vol) sucrose, and 0.1% ampholine (pH 3.5 to 8) (LKB) and applied to sucrose gradients (10 to 40%) generated with a Beckman density gradient former. Between 100 and 200 μl of sample was layered onto the gradient and subsequently spun in a Beckman SW60 rotor at 58,000 rpm for 18 h at 3°C. Thirteen-drop samples were collected from the bottoms of the punctured tubes and assayed for DNA binding and DNA polymerase δ activities. Calibration markers of ferritin (440 kDa), catalase (232 kDa), aldolase (158 kDa), ovalbumin (44 kDa), and myoglobin (17 kDa) were sedimented in parallel gradients for size estimations.

**Immunoblotting.** Fractions from the sucrose gradient (75 μl) were resolved on a sodium dodecyl sulfate (SDS)–7.5% polyacrylamide gel by the method of Laemmli (22) and transferred to an Immobilon-P membrane (Millipore Corp.) as suggested by the supplier. Nonspecific protein binding was blocked with 1% nonfat dry milk in PBS overnight at 4°C. Following application of the primary anti-RPA antibody (p70-9), reactive protein was visualized using the Vectastain alkaline phosphatase kit (Vector Laboratories) with nitro-blue tetrazolium–5-bromo-4-chloro-3-indolylphosphate tolu-idinium indicator for detection as suggested by the supplier.

**Gel mobility shift assays.** Gel mobility shift assays were performed by incubating 5 μg of the cell extract with $10^4$ cpm of the radiolabeled oligonucleotide (10 to 20 fmol) in 50 mM HEPES-KOH (pH 7.5)–150 mM NaCl–1 mM EDTA–5 mM DTT–10% glycerol in the presence of 2 μg of poly(dI · dC) (Pharmacia LKB) for 30 min at room temperature. Other competitor DNAs or antisera were included in the reaction mixture as indicated in Results. The poly(dI · dC) (Pharmacia) was added as nonspecific competitor DNA to all gel retention assays at an ~$10^5$-fold molar excess over labeled target DNA to reduce nonspecific binding. In some experiments, an additional $10^3$-fold excess of single-stranded M13 DNA was added to remove RPA binding. DNA-protein complexes were resolved from free DNA on prerun 4% polyacrylamide gels in Tris-glycine-EDTA buffer (50 mM Tris, 380 mM glycine, 2 mM EDTA), maintained at 4°C by recirculating refrigeration.

**UV cross-linking.** UV cross-linking of protein to DNA was performed as described by Chodosh et al. (9) with the following modifications. Protein-DNA binding reactions were performed in 96-well plates exactly as described for the

**A**

```
              G
            /   \
            C--G
            G--C
            G--C
            A--T   T-Ag binding site II
            G--C
        ∧   C--G
     T   G  C--G
     C--G  G G--C
     T--A    G--C
   C T--A    A--T
    \A--T    G--C   A/T region (17 bp)
     T--A    A--T
5'-AAGCCTAGGCCTCCAAAAAAGCCTCCTCAC--GCTC--GCATAAATAAAAAAAATTAGTCAGC
  T-Ag binding site I
                                    Core origin (65 bp)
                                    5229
5206
```

```
        5206                                    5229
SV40    C T C C T C A C T A C T T C T G G A A T A G C T

        *   * * *   * * *     *     *     *
EBV       C T A A C C C T A A T T C G A T A G C A T A T

        * * *   *   * * * * *       * * * *       *
HSV-1   C T C G C - A C T T C C C T A A T A A A T
                    C G

        * *   * * * * * * * * *       * * * *
JCV     C T T A C T A C T T C T G A G T A A G C T

        * *   * * * * * * *     *     * * *
BKV     C T T A C T A C T T G A G A G A A A G G G

        * *   * * * * * * * * *         * *
SA 12   C T T A C T A C T T C T A A G C A A G G G
```

**B**

**IR1**    5'-CTCCTCACTACTTCTGGAATA-3'
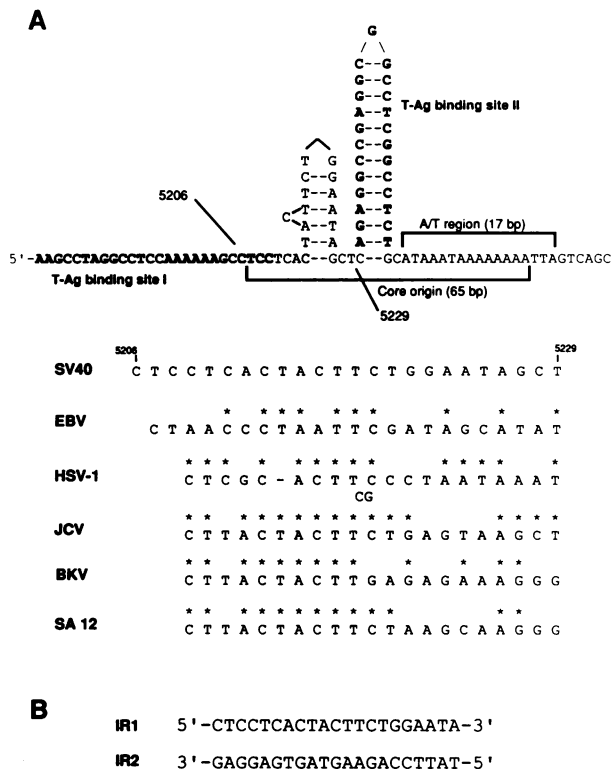
**IR2**    3'-GAGGAGTGATGAAGACCTTAT-5'

FIG. 1. (A) Schematic of the SV40 minimal origin and nucleotide sequence conservation between several mammalian viral origins of replication. The nucleotide sequence of the SV40 IR domain (nucleotides 5206 to 5229) is compared with regions in the origins of replication in EBV oriP (2), BK virus (BKV) (12), JC virus (JCV) (18) and herpes simplex virus type 1 oriS (HSV-1) (47). Sequences identical to the SV40 sequence are denoted by asterisks. (B) Oligonucleotide sequences used in this study. The oligonucleotide IR2 sequence begins at the SV40 nucleotide position 5226 (shown in panel A). Oligonucleotide IR1 is its complement. T-Ag, T antigen.



FIG. 2. UV-induced IR domain binding activities in HeLa cell extracts. Nuclear and cytosolic extracts from HeLa cells treated with 0, 3, and 6 J/m² were prepared 1 h after treatment as described in Materials and Methods. Five micrograms of each extract was incubated with ³²P-labeled IR1–IR2 oligonucleotides (Fig. 1B), and DNA-protein complex formation was analyzed by gel mobility shift assay. A and B, IRF-A and -B complexes, respectively.

gel mobility shift assays. Immediately following the 30-min incubation, the reaction mixture was subjected to 0.8 J of UV radiation per s for 10 min in a Stratalinker (Stratagene). SDS-polyacrylamide gel electrophoresis (PAGE) sample buffer was added to the reaction mixture and boiled for 5 min prior to loading onto a SDS–12% polyacrylamide gel. Resolved complexes were visualized by autoradiography and quantitated by phosphorimage analysis (Molecular Dynamics Phosphorimager).

## RESULTS

**IR domain binding is responsive to UV irradiation.** To characterize cellular factors binding the IR domain, we examined DNA binding in response to cellular DNA damage. Logarithmically growing HeLa cells were irradiated with 254-nm UV light doses of 0, 3, and 6 J/m². Cytosolic and nuclear protein fractions, prepared and quantitated 60 min after UV treatment, were used in a gel mobility shift assay. The sequences of SV40 IR domain DNA oligonucleotides used in these studies are shown in Fig. 1B. Complementary SV40 IR oligonucleotides IR1 and IR2 were prepared, labeled, and annealed at equimolar ratios as described in Materials and Methods. Gel shift assay of labeled IR1–IR2 oligonucleotides with nuclear or cytosolic extracts from
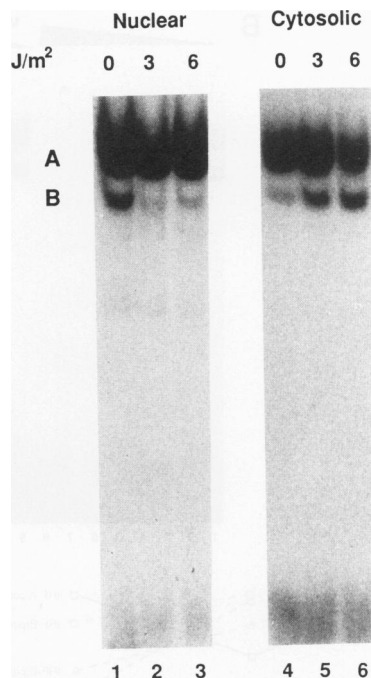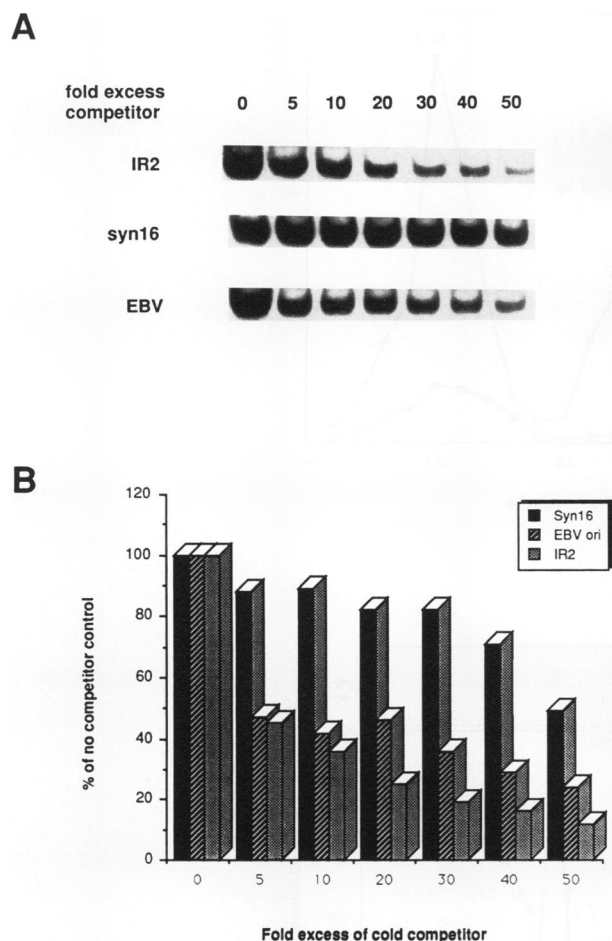
untreated HeLa cells resulted in two major protein-DNA complexes (Fig. 2, lanes 1 and 4, respectively). The protein component of the more slowly migrating complex is referred to as IRF-A, and that of the faster-migrating complex is referred to as IRF-B. Consistent with the results of Lücke-Huhle et al. (28), UV doses of 3 and 6 J/m² enhanced IRF-B binding activity in cytosolic extracts (Fig. 2, lanes 5 and 6). However, the binding activity of IRF-B from nuclear extracts diminished in response to UV treatment (Fig. 2, lanes 2 and 3). The binding activity of IRF-A was nominally affected in both cytosolic and nuclear extracts in response to UV treatment.

**IRF-A and IRF-B bind opposite strands of the SV40 IR domain.** To assess whether IRF-A or IRF-B binding activities are specific for double or single strands of the IR domain, gel shift assays were performed with either single-stranded IR1 or IR2 DNA probes (Fig. 3A). Incubation of 5 μg of proliferating HeLa cell nuclear extracts with each of the single-stranded probes resulted in different levels of IRF-A and -B complexes. Oligonucleotide IR1 yielded predominantly the more slowly migrating IRF-A complex. In contrast, the higher-mobility complex, IRF-B, was predominantly observed with oligonucleotide IR2. When a 10⁵-fold molar excess of poly(dI · dC) was used as the only competitor, the IR2 probe also showed small amounts of IRF-A complex in addition to the predominant IRF-B complex. This suggested that IRF-A is not sequence specific but is preferential to IR1.

To further define sequence-specific interactions of IRF-A and -B with single-stranded IR2 DNA only, gel shift with labeled IR2 DNA and nuclear extract was performed in the

FIG. 3. Sequence specificity of IR domain oligonucleotide binding by host factors IRF-A and IRF-B. (A) Gel mobility shift analysis with 5 μg of nuclear extract binding to single-stranded oligonucleotides IR1 and IR2 was performed as described in Materials and Methods. (B) Competition for binding of nuclear protein to single-stranded IR2 DNA was performed in the presence of increasing concentrations of unlabeled IR2 (50×, 100×, 200×, 400×, 800×, 1,600×, and 3,200× molar excesses [lanes 2 through 8, respectively]) or single-stranded M13mp18 (125×, 250×, 500× and 1,000× molar excesses [lanes 10 through 13, respectively]) in addition to the poly(dI · dC) DNA included in all assays. Lanes 1 and 9 contain only poly(dI · dC) as the unlabeled competitor. A and B, positions of IRF-A and IRF-B complexes, respectively. (C) Binding of nuclear protein to single-stranded IR1 and IR2 oligonucleotides was performed in the presence of increasing concentrations of unlabeled poly(dA), poly(dT), or single-stranded M13mp18 DNA. The radioactivity within the IRF-A and -B gel shift complexes on the gel in the presence of increasing concentrations of competitor was directly quantitated using a Betascope analyzer (Betagen), and the results were plotted as percentages of the amounts of radioactivity in complexes formed in the absence of cold competitor DNA (% of control). Solid lines, IRF-A–IR1 complex; dotted lines, IRF-B–IR2 complex. The competitors poly(dA), poly(dT), and M13mp18 are represented by squares, triangles, and circles, respectively.

presence of increasing levels of unlabeled IR2 DNA or single-stranded phage M13mp18 DNA, in addition to the poly(dI · dC) present in all binding assays (Fig. 3B). The unlabeled IR2 oligonucleotide effectively competed for labeled IRF-B binding at low concentrations (50-fold molar excess). In contrast, a 400-fold molar excess of unlabeled

IR2 competitor was required to compete for IRF-A binding. An additional $10^3$-fold molar excess of M13mp18 single-stranded DNA effectively eliminated the interaction of IRF-A with IR2 (Fig. 3B, lane 13) with no effect on the IRF-B–IR2 interaction. This allowed us to examine the specific interaction of IRF-B with IR2 DNA shown in subsequent experiments. These results demonstrate that IRF-B binds to the IR2 sequence with much greater specificity than does IRF-A.

We have also tested an 80-bp restriction fragment containing the SV40 IR domain duplex in competition studies with IR2, and it was not an effective competitor for binding (data not shown). Although the 20-mer oligonucleotides IR1 and IR2 derive from the SV40 IR domain, on the basis of the low theoretical melting temperature calculated for potential base pairing within the molecules, each alone is unlikely to form a stable duplex DNA structure because of intra- or intermolecular base pairing. Therefore, the IRF-A and -B factors do not appear to be binding a double-stranded component of either oligonucleotide. Likewise, because it derives from inverted repeats, the annealed duplex IR1–IR2 used in the initial studies (Fig. 2; see also Fig. 5) appears to be sufficiently unstable at 37°C in the presence of both factors to provide some single strands of each in the mobility shift. The same patterns of gel shift were obtained when annealed DNA was added or combined labeled strands were added to the binding reaction (data not shown).

Results from gel mobility shift assays suggested that IRF-A binds preferentially to IR1, with some residual binding to IR2 (Fig. 3A), and high concentrations of M13mp18 can eliminate IRF-A–IR2 interaction (Fig. 3C). Since IR1 is rich in pyrimidines (67%), we reasoned that IRF-A may complex preferentially to pyrimidine-rich DNA. The base composition preference of IRF-A was tested in a IR1 DNA gel shift with either polypurine DNA [poly(dA)] or polypyrimidine DNA [poly(dT)] as a competitor (Fig. 3C). Poly(dT) and M13mp18 effectively competed for binding of IRF-A to labeled IR1, whereas poly(dA) did not. When IR2 DNA was used as the labeled probe, these competitors minimally affected the IRF-B–IR2 complex. On the basis of these results, we conclude that IRF-A is a single-stranded binding protein with a preference for pyrimidine-rich DNA. However, IR1 is three times more efficient than poly(dC) in competing for IRF-A binding (data not shown), suggesting some sequence specificity. Importantly, the second single-stranded binding component, IRF-B, appears to be IR2 sequence specific, and a 1,000-fold molar excess of either polypurine or polypyrimidine DNA does not effectively compete for the IRF-B–IR2 interaction (Fig. 3C).

To further demonstrate the IR2 sequence specificity of IRF-B, we examined IR2–IRF-B binding in competition with other DNA oligonucleotides of the same size in mobility shift experiments. As expected, the addition of a 50-fold molar excess of unlabeled IR2 oligonucleotide to the binding reaction mixture diminished complex formation by 90% (determined by the number of counts per minute in the shifted band) (Fig. 4). The addition of a 50-fold molar excess of a nonspecific competitor, the syn16-1 fragment of a hepatocyte-specific cis-acting element (28, 45), diminished the IRF-B complex by only 49%. A 50-fold molar excess of the Epstein-Barr virus (EBV) oriP fragment (nucleotides 8922 to 8944), containing sequence homology to SV40 IR2 (Fig. 1), in the binding reaction mixture diminished binding by 76% (Fig. 4).

**Partial purification of IRF-A and -B.** To further characterize the SV40 IR binding factors, S100 extract from HeLa

**A**



**B**



FIG. 4. IR2 DNA binding activity in the presence of oligonucleotide competitors. (A) Gel mobility shifts of IR2 in the presence of increasing concentrations of cold IR2, syn16-1 oligonucleotide, (syn16), or EBV oligonucleotide (EBV ori) were performed. The resultant IR2–IRF-B complexes are shown. (B) The radioactivity within the IRF-B complexes on the gel (A) were directly quantitated with a Betascope analyzer (Betagen), and the results were graphed. The bars represent the percentage of counts per minute per band (with the value for no competitor taken as 100%).

cells was chromatographed on sequential S Sepharose and Q Sepharose resins as described in Materials and Methods. The IRF-A and -B components are detectable in both cytosol and nuclear extracts, and for convenience, cytosol was used for initial purification. Column fractions 12 to 20 off Q Sepharose (Fig. 5A) contained DNA polymerase δ activity, detectable on a synthetic poly(dA) · oligo(dT) template. Assignment of specific DNA polymerase activities in column fractions were based on synthetic template and nuclease specificity, as well as drug and antibody sensitivity as previously reported (19, 48, 55) (see the legend to Fig. 5). Gel mobility shift assay performed with SV40 IR DNA (annealed strands) and column elution fractions from Q Sepharose revealed that the IRF-A and IRF-B factors coelute with DNA polymerase δ activity. Gel filtration of the DNA polymerase δ-IRF-containing fractions over a calibrated Superose-6 column at physiological salt concentrations, followed by DNA polymerase and gel mobility shift assays, indicated that the factors are not well resolved from DNA polymerase δ activity. IRF-A, DNA polymerase δ, and

IRF-B activities gel filter to ca. 215, 220, and 225 kDa, respectively (data not shown). The IRF-A binding activity and DNA polymerase δ were resolved from IRF-B binding activity by subsequent AMP-Sepharose chromatography (Fig. 5B). This method has been previously shown to be an effective affinity ligand for DNA polymerase δ via its associated 3′-to-5′ exonuclease (11). Post-Q Sepharose fractions containing DNA polymerase δ and IRF activities were pooled, concentrated on S Sepharose, and loaded onto a column of AMP-Sepharose as described in Materials and Methods. Fractions of unbound material and the 350 mM KCl-eluted retentate were assayed for DNA polymerase δ activity, polymerase-associated 3′-to-5′ exonuclease activity, and SV40 IR domain binding activities (Fig. 5B). IRF-B activity was detected in flowthrough fractions from this column, whereas polymerase δ, δ nuclease, and IRF-A activities were coeluted by the 350 mM KCl wash.

The IRF-B active fractions also contained minor polymerase activity. This material was not retained by a second column passage, and the lack of nuclease activity suggests that it is not DNA polymerase δ. We are further characterizing this activity.

**Identification of IRF-A as RPA.** DNA polymerase δ and IRF-A activities from AMP-Sepharose were further resolved by preparative sedimentation through a 10 to 40% sucrose gradient. Consistent with prior reports (11), DNA polymerase δ sedimented to a position corresponding to 220 kDa. IRF-A activity was resolved by several fractions from DNA polymerase activity and sedimented to a position corresponding to ca. 120 kDa (Fig. 6B). Aliquots of samples through the sucrose gradient were resolved by SDS-PAGE, and proteins were visualized by silver staining (data not shown). The major protein bands which increase and decrease in intensity coincident with IRF-A activity had molecular masses of 70 kDa (48 kDa), 32 kDa, and 15 kDa. The 48-kDa protein increased with time and storage after isolation and appears to be a proteolytic fragment of the larger subunit. Western blot (immunoblot) analysis with a monoclonal antibody directed against the 70-kDa subunit of RPA (14) revealed a 70-kDa immunoreactive protein (Fig. 6A) that is maximal, coincident with the peak of IRF-A–IR1 binding (Fig. 6B). To examine the functional contribution of RPA to the IRF-A binding activity, we performed IR1 gel mobility shift assays in the presence of anti-RPA IgG (Fig. 6C). The addition of anti-RPA monoclonal antibody resulted in the appearance of a more slowly migrating complex above the IRF-A,A′ (Fig. 6C, lane 2). Titration with increasing amounts of anti-RPA resulted in total conversion to the more slowly migrating complex (data not shown). The loss of the IRF-A band and appearance of a lower-mobility species in the presence of anti-RPA suggests that the 70-kDa subunit of RPA is the active component of IRF-A. In control experiments, the addition of monoclonal antibodies directed against p53 (Fig. 6C, lane 4), retinoblastoma protein (lane 5), T antigen (lane 6), and heat shock protein 70 (lane 7) to the binding reaction mixture did not perturb the formation of the IRF-A (RPA)-containing complex.

**Changes in IRF-B binding activity during cell proliferation and the cell cycle.** Because UV irradiation modulates both IRF-B binding to IR2 (Fig. 2) and induction of SV40 DNA replication (15, 25–27, 29, 44) in vivo and in vitro (4), we asked whether nuclear IRF-B binding activity changes during onset of scheduled DNA replication. The use of excess competitor DNA in the gel shift assay enabled specific examination of the IR2 binding by IRF-B in nuclear extracts. Normal human lung fibroblast IMR90 cells were grown to
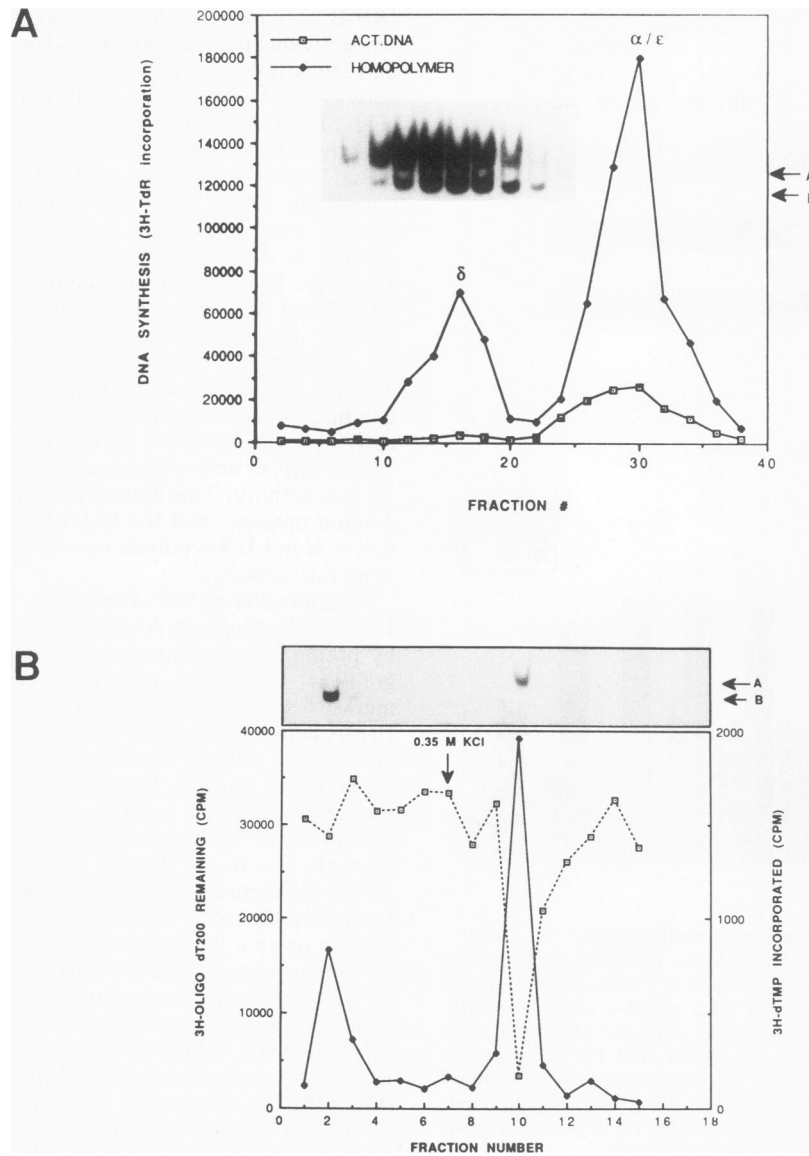
FIG. 5. Partial purification of factors binding to the IR domain oligonucleotides. (A) HeLa cytosolic extract was enriched for DNA polymerase activity by chromatography over S Sepharose, followed by chromatography over Q Sepharose developed with a 100 to 400 mM NaCl linear gradient as described in Materials and Methods. DNA polymerase α, δ, and ε assays were performed with activated calf thymus DNA (ACT.DNA) or poly(dA) · oligo(dT) templates (HOMOPOLYMER) (19). Fractions were also assayed for IR binding activity by gel mobility shift with both IR1 and IR2 probes. The arrows denote shifted complexes IRF-A and -B present in fractions 12 through 20. TdR, thymidine. (B) Post-Q Sepharose fractions 12 through 20 were pooled, concentrated on S Sepharose, and further fractionated by AMP-Sepharose chromatography. The position where 350 mM KCl elution buffer was applied to the column is indicated on the graph. DNA polymerase δ activity (solid line) and its associated 3'-to-5' exonuclease activity (broken line) were assayed from each fraction and plotted. The gel mobility shift assay from each fraction with both IR1 and IR2 probes is shown above the graph. Arrows A and B denote IRF-A and IRF-B complexes, respectively. The polymerase activities contained in Q Sepharose fraction 16 and AMP-Sepharose fraction 10 were inhibited >97% by 5 μg of aphidicolin per ml, insensitive to 2 μg of SJK 132-20 (anti-DNA polymerase α) IgG per ml, and inhibited 58 and 60%, respectively, by 10 mM BuPdGTP.

confluence and deprived of serum for 5 days to bring about quiescence. Upon restimulation of growth by trypsinization and addition of fresh serum-containing medium, cells synchronously progressed from the $G_0$ (or quiescent) stage through initial stages of cell proliferation and initiation of DNA synthesis. Figure 7A shows the DNA synthesis profile, as determined by [$^3$H]thymidine incorporation in equal numbers of cells, at various times after serum stimulation. The profile of IRF-B binding activity in 5 μg of nuclear extract

made from cells at each time is shown below the graph. During quiescence ($G_0$), IRF-B activity is abundant in nuclear extracts. However, at the onset of DNA replication (20 h after restimulation), IRF-B binding activity is minimal in nuclear extracts and is then reestablished during DNA synthesis.

It is not clear from the serum starvation studies whether the IRF-B activity is diminished as the result of stimulation to proliferate or is dependent on initiation of DNA synthesis.
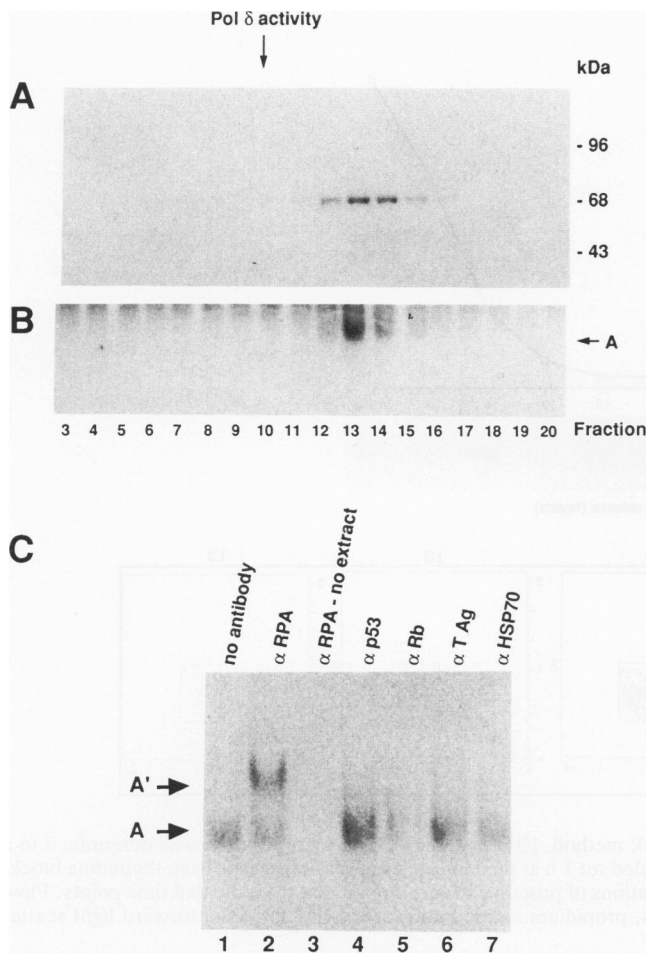
FIG. 6. Western blot and gel mobility shift analysis of IRF-A with anti-RPA IgG. (A) The fraction of peak AMP-Sepharose retained IRF-A activity was sedimented through a 10 to 40% sucrose gradient as described in Materials and Methods. Samples from each fraction were electrophoresed on an SDS–7.5% polyacrylamide gel and transferred to polyvinylidene difluoride paper, and Western blot analysis was performed with the anti-RPA monoclonal antibody p70-9. Molecular mass markers are shown on the right. The fraction that contained peak polymerase δ (Pol δ) activity is indicated at the top of the figure. (B) Sucrose gradient fractions were also analyzed in a gel mobility shift assay with the single-stranded IR1 DNA probe. The presence of the IRF-A complex is indicated. (C) A gel mobility shift assay of IR1 probe was performed in the presence of no antibody (lane 1), anti-RPA antibody p70-9 (lane 2), anti-RPA antibody p70-9 in the absence of HeLa extract (lane 3), anti-p53 clone 421 (lane 4), anti-Rb clone C36 (lane 5), anti-T-antigen (T-Ag) antibody PAb 419 (lane 6), and anti-heat shock protein 70 (HSP70) antibody SPA-820 (lane 7). The RPA-DNA and anti-RPA–RPA-DNA complexes are denoted by A and A′, respectively.



FIG. 7. Cell proliferation and cell cycle regulation of IRF-B complex formation. (A) IMR90 cells were brought to quiescence by serum starvation and stimulated to proliferate by the addition of medium containing 10% fetal bovine serum. Gel mobility shift analysis of the IR2 DNA probe was performed with 5 μg of nuclear extracts prepared at the indicated times after serum stimulation of resting IMR90 cells. Cellular DNA synthesis was monitored by [³H]thymidine incorporation in equal cell numbers from each population. (B) MANCA cells were synchronized by centrifugal elutriation, and [³H]thymidine incorporation was determined with equal cell numbers from each population to verify progression through the cell cycle. Gel mobility shift analysis was performed with 5 μg of nuclear extract prepared from each population and end-labeled IR2 oligonucleotide.

To examine the cell cycle regulation of IRF-B activity, logarithmically growing MANCA cells were separated into the progressive stages of the cell cycle by counterflow centrifugal elutriation (Fig. 7B) (31). This procedure does not perturb cellular metabolism and separates proliferating cells on the basis of the regular increase in cell mass and cell volume that occurs during progression through the cell cycle. MANCA cells were selected for these experiments because their substantial size increase during the cell cycle permits efficient separation. Coulter cell volume analysis of

subpopulations 1, 4, and 6 showed an approximate volume ratio of 1.0:1.6:2.1, respectively. Flow cytometry for DNA content was performed with all successive subpopulations to determine the progressive stages of the cell cycle (data not shown). Flow cytometry analysis for DNA content indicated average purities of 93, 87, and 82% for subpopulations 1, 4, and 6, respectively. Early $G_1$ fractions could not be obtained with acceptable purity, and the first fractions off the elutriator were not used for this study. Measurement of [³H]thymidine incorporation from equal numbers of cells from each population indicated the onset, peak, and decline of cellular DNA synthesis through the cell cycle (Fig. 7B). Nuclear
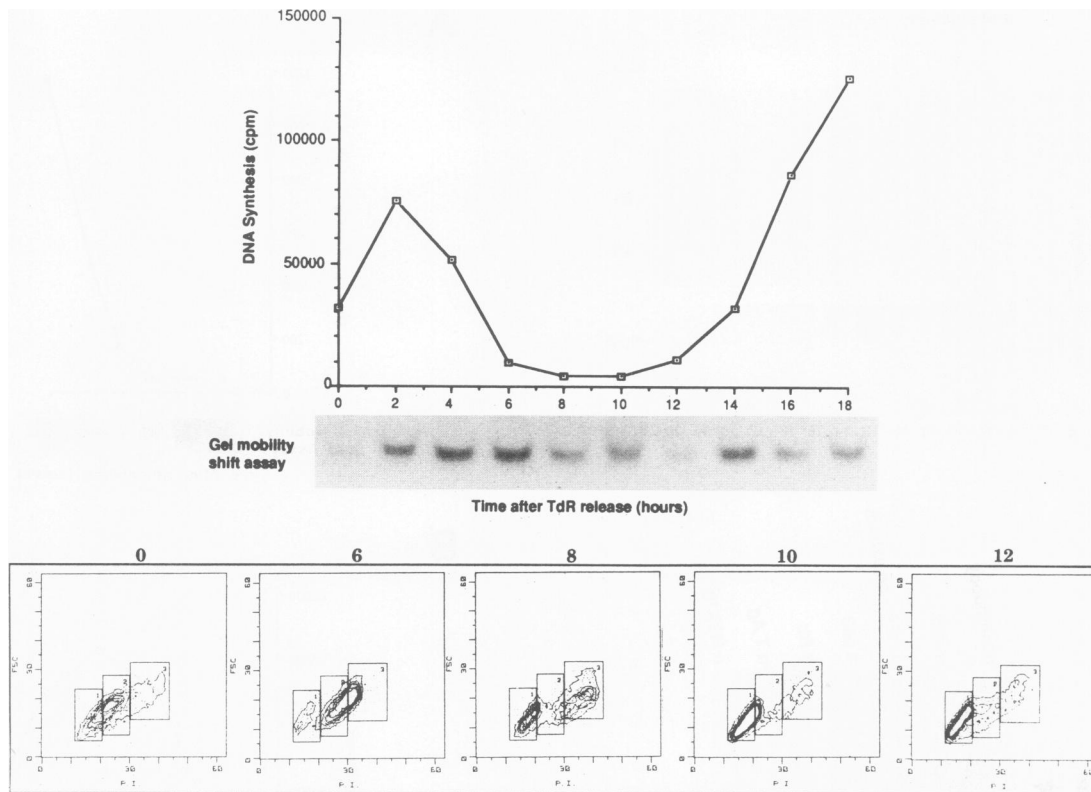
FIG. 8. HeLa cells were synchronized by the double thymidine block method. [³H]thymidine (TdR) incorporation was determined in a parallel 24-well plate seeded at $5 \times 10^5$ cells per well at time zero and labeled for 1 h at the indicated times after release from thymidine block. Gel mobility shift assay with IR2 DNA was performed on equal concentrations of protein extracts prepared at the indicated time points. Flow cytometry was performed on fractions from 0, 6, 8, 10, and 12 h. $x$ axis, propidium iodide fluorescence (P.I.); $y$ axis, forward light scatter (FSC). Cell division occurs at ~ 8 h.

extracts were prepared from these populations, and 5 μg of each extract were analyzed for IRF-B activity by gel mobility shift analysis of the IR2 DNA. Figure 7B shows the DNA gel mobility shift and the [³H]thymidine incorporation profile for each fraction. Consistent with the serum stimulation profile, IRF-B activity is nominally detectable prior to the onset of DNA synthesis and is present throughout the remainder of the cell cycle.

To verify these data and to address whether IRF-B activity is present in proliferating early $G_1$ populations, we examined IRF-B activity in HeLa cells that were synchronized by double thymidine block. Elevated levels of deoxyribonucleosides inhibit DNA synthesis, causing cells to arrest at the $G_1$/S-phase boundary (49). Upon removal of excess thymidine, cells synchronously complete the remainder of the cell cycle and initiate another cell division cycle. Synchronized HeLa cells were released from double thymidine block, DNA synthesis was monitored, and extracts were prepared every 2 h thereafter for a complete cell division cycle (S-phase through subsequent S-phase). Flow cytometry data indicated that cell division occurred at ~8 h postrelease (Fig. 8). DNA synthesis, determined by [³H]thymidine incorporation, initiated immediately after release and for the second cell division cycle at 12 h after release. Five micrograms of nuclear extract from each fraction was assayed for IRF-B binding activity. As shown in Fig. 8, the extracts prepared from thymidine-blocked cells ($T = 0$) and

from the cells released for 12 h exhibited minimal levels of IRF-B activity.

**IRF-B contains a 34-kDa component.** To further characterize the DNA binding component in the IRF-B complex, UV cross-linking experiments were performed on nuclear extracts from the thymidine-synchronized cells. This method identifies only those proteins in contact with DNA that can be cross-linked with UV irradiation. IR1 and IR2 probes were separately combined with 5 μg of nuclear extracts obtained from either cells with reduced IRF-B activity ($T = 0$ or 12 h after thymidine release) or those containing IRF-B activity ($T = 2$ or 10 h after thymidine release) and UV cross-linked as described above. Protein-DNA complexes were resolved by SDS-PAGE and visualized by autoradiography (Fig. 9A). UV irradiation of IR1 DNA with nuclear extracts identifies a protein of ca. 70 kDa (probably the 70-kDa subunit of RPA). Consistent with gel shift data, UV cross-linking of nuclear extracts with IR2 DNA identifies a protein of ca. 34 kDa that is diminished in extracts of cells at the onset of DNA synthesis (Fig. 9A, $T = 0$ and 12 h). Southwestern (DNA-protein) analysis of nuclear extract has also confirmed the IR2-specific DNA binding by a renatured 34-kDa protein (data not shown).

Titration of MANCA cells with the DNA-damaging agent MNNG ultimately results in the loss of IRF-B binding to IR2 DNA with no effect on RPA binding to IR1 (8a). Gel mobility shift assay revealed no IRF-B activity in nuclear extracts

# A



# B



# C
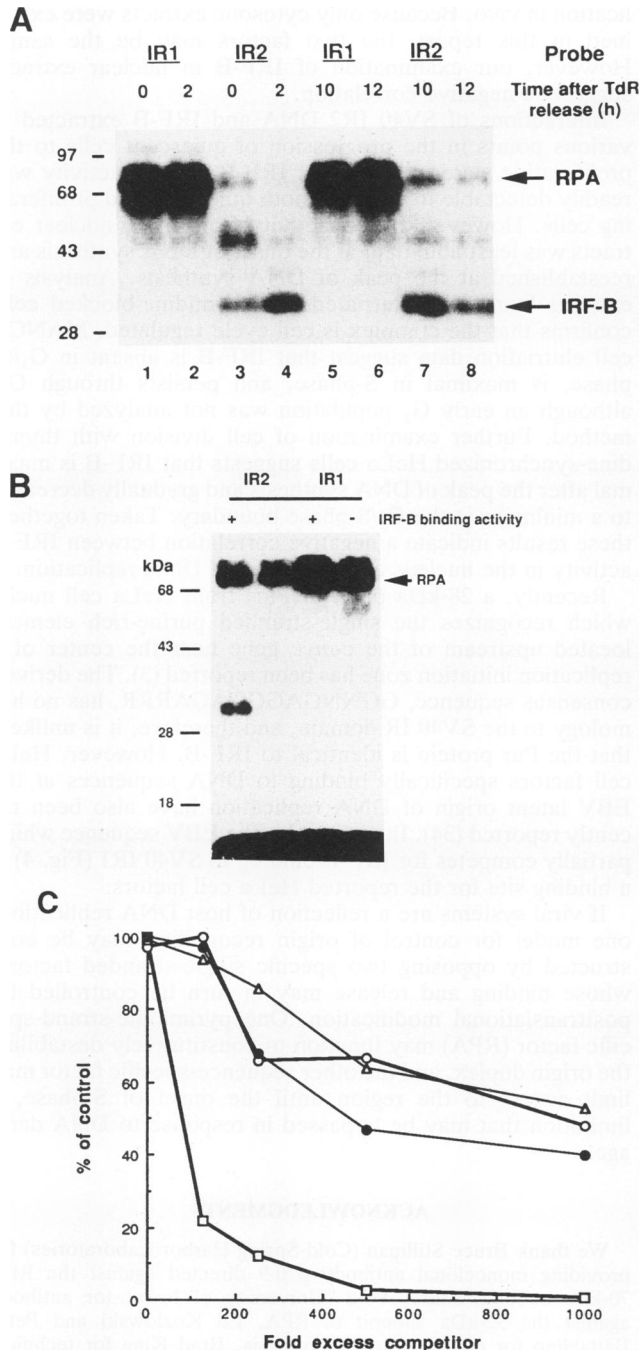


FIG. 9. Analysis of the IRF-A and -B components by UV cross-linking. (A) Nuclear extracts from thymidine (TdR)-blocked cells (lanes 1 and 3) and from cells released from thymidine block for 2 h (lanes 2 and 4), 10 h (lanes 5 and 7), and 12 h (lanes 6 and 8) were utilized in a binding reaction with IR1 or IR2 DNA probes as indicated. The binding reactions were UV irradiated to cross-link DNA-protein complexes. Following UV treatment, the resulting complexes were resolved by SDS–12% PAGE and visualized by Betascope Image Analyzer (Betagen). Molecular weight standards (in thousands) are indicated on the left. The 70-kDa component of RPA and the DNA binding component of IRF-B are indicated with arrows. (B) Nuclear extracts (5 μg) from untreated MANCA cells (lanes 1 and 3) or from MANCA cells treated with 7 μg of MNNG per ml (lanes 2 and 4) were utilized in a binding reaction with either IR1 or IR2 DNA probes, UV cross-linked, and visualized as described above. The presence (+) or absence (−) of IRF-B gel shift

prepared from cells treated with 7 μg of MNNG per ml. Nuclear extracts from untreated and treated cells were combined with IR1 or IR2 probes, UV irradiated to cross-link DNA and protein, and resolved and visualized as described above (Fig. 9B). In the presence of only excess dI · dC DNA as a competitor, a major band of ca. 70 kDa was observed with treated or untreated nuclear extracts with either IR1 or IR2 as the probe (Fig. 9B); as expected, the 70-kDa band was more prominent with IR1 probe. When IR2 was used as the probe, a major band of ca. 34 kDa was observed in untreated nuclear extract (Fig. 9B, lane 1). In contrast, extracts of MNNG-treated cells contained no detectable IR2–34-kDa complex (Fig. 9B, lane 2). The IR1 probe revealed no 34-kDa binding activity. This stable association is dependent on extended UV irradiation; in the absence of UV crosslinking, neither band was observed and no protein was detected associated with the DNA probe after reducing SDS-PAGE. To further assess the specificity of interaction of labeled IR2 DNA with a 34-kDa protein, UV cross-linking of MANCA cell nuclear extract with IR2 DNA probe was repeated in the presence of increasing levels of unlabeled IR2 or syn16-1 DNA. The cross-linked products were resolved as described above, the radioactivity within the 34-kDa protein-DNA complexes was directly quantitated with a phosphorimage analyzer, and the results were graphed (Fig. 9C). The addition of a 125-fold molar excess of cold IR2 DNA diminished the 34-kDa signal by 82%; however, addition of a 125-fold molar excess of syn16-1 did not efficiently compete for the 34-kDa protein. UV light cross-links a 70-kDa protein (RPA in Fig. 9B) to the IR2 probe, and this is also affected by the two competitors. Syn16-1 is a more effective competitor for RPA, possibly because of its high pyrimidine content (53%) compared with that of IR2 (33%).

## DISCUSSION

One consequence of cellular DNA damage is productive viral DNA replication in infected cells and amplification of genomic sequences in transformed cells (1, 22, 25, 26, 44, 50). Activation of unscheduled DNA synthesis has been related to binding of uncharacterized viral-origin recognition factors (28, 40). We have utilized gel mobility shift assays in the presence of excess competitor DNA to characterize two binding activities which interact specifically with opposite strands of the IR domain of the SV40 core origin of replication. This sequence is conserved in many viral origins, and in SV40, it has been shown to be the initial site of origin melting prior to the onset of DNA synthesis (6, 35). On the basis of competition and gel mobility shift analysis with each strand of the SV40 IR domain, there appear to be two protein

is indicated. (C) UV cross-linking of IR2 DNA to the 34-kDa protein in the presence of oligonucleotide competitors. Nuclear extracts (5 μg) from untreated MANCA cells were utilized in a binding reaction with IR2 DNA probe and increasing levels of unlabeled competitor, and the reactants were UV cross-linked and resolved as described above. The radioactivity in the resulting 34- or 70-kDa bands were qauntitated by phosphorimage analysis and plotted as the percentage of the counts per minute per band obtained with no competitor. UV cross-linking of IR2 to the 34-kDa protein in the presence of unlabeled IR2 DNA (□) and syn16-1 DNA (○) is shown. UV cross-linking of the 70-kDa protein (RPA in panel B) to the IR2 probe is also successfully competed against by addition of unlabeled IR2 DNA (△) or syn16-1 DNA (●) and is shown as a control.

complexes which bind to opposite strands of the origin DNA. IRF-B has high sequence specificity to the IR2 single strand, and IRF-A (RPA) preferentially binds to the pyrimidine-rich IR1 strand (Fig. 3).

Characterization of IRF-A by SDS-PAGE and Western blot analysis is consistent with its being RPA (previously called RF-A or HSSB [16, 57, 58]). RPA is a single-stranded DNA binding protein essential for in vitro SV40 DNA replication, and its preference for binding pyrimidine-rich DNA has recently been reported (20). Our studies have identified RPA by its preferential affinity for the pyrimidine-rich strand of the SV40 IR domain. Gel shift with RPA and IR1 DNA can be successfully competed against with excess polypyrimidine or single-stranded M13 DNA, whereas polypurine DNA is unable to efficiently compete for binding. In contrast, use of both excess dI · dC and single-stranded M13 DNAs with the IR2 probe showed only the specific interaction of IR2 DNA with IRF-B (Fig. 3). The RPA protein complex has been shown to be modified in a cell cycle-dependent manner, with phosphorylation occurring at the $G_1$/S-phase transition and dephosphorylation at $G_2$/M (14). Because RPA appears to be constitutively active in binding IR1 and present in the nucleus under all conditions tested, phosphoregulation may control the ability of RPA to interact with other replication proteins rather than its interaction with DNA.

The factors RPA and IRF-B copurify with DNA polymerase δ through the initial stages of purification and gel filtration under physiological conditions but can be resolved by subsequent chromatography over AMP-Sepharose and sucrose gradient sedimentation. RPA has components of 70, 32, and 14 kDa (59), and our sedimentation data indicate a molecular mass of ca. 120 kDa for the RPA complex. However, separation of post-Q Sepharose material by Superose-6 chromatography under physiological salt indicated that RPA and IRF-B gel filter at apparent molecular masses of 215 and 225 kDa, respectively. Whereas IRF-B activity from nuclear extracts gel filters to an apparent molecular mass of ca. 225 kDa, the ca. 34-kDa protein identified by UV cross-linking likely represents the active component of a larger complex. To address the possibility that RPA also participates in the IRF-B complex, we have performed similar experiments with IRF-B and the anti-RPA p70 and anti-RPA p32 antibodies. Using these reagents, we have not seen immunoreactivity after AMP-Sepharose chromatography and Western blotting that is coincident with IRF-B activity, nor have we seen any change in the mobility of the IRF-B–IR2 gel shift in the presence of these antibodies (data not shown). On the basis of these results, we have no evidence to suggest that RPA or one of its subunits is a component of the IRF-B complex. The possibility of direct interaction of these two factors is currently under investigation.

UV treatment has no effect on RPA binding or its intracellular partitioning. In contrast, UV exposure reduces the level of IRF-B present in the nucleus, with a concomitant increase in IRF-B in the cytosol (Fig. 2). Lücke-Huhle et al. (28) have reported that the level of a factor(s) binding the SV40 IR domain increases in cells in response to UV radiation and DNA damage and have correlated this increase with increased viral DNA replication (28). The introduction of SV40 IR domain oligonucleotides into cells inhibited DNA amplification, presumably by binding and sequestering the DNA damage-activated factor (28). They concluded that binding of a cytosolic factor to the SV40 IR domain is an absolute requirement for the UV-induced SV40 DNA ampli-

fication in vivo. Because only cytosolic extracts were examined in this report, the two factors may be the same. However, our examination of IRF-B in nuclear extracts suggests a negative correlation.

Interactions of SV40 IR2 DNA and IRF-B extracted at various points in the progression of quiescent cells to the proliferative state indicate that IRF-B binding activity was readily detectable in nuclei of both quiescent and proliferating cells. However, IRF-B activity from these nuclear extracts was least abundant at the onset of DNA synthesis and reestablished at the peak of DNA synthesis. Analysis of extracts from both elutriated and thymidine-blocked cells confirms that the complex is cell cycle regulated. MANCA cell elutriation data suggest that IRF-B is absent in $G_1$/S-phase, is maximal in S-phase, and persists through $G_2$, although an early $G_1$ population was not analyzed by this method. Further examination of cell division with thymidine-synchronized HeLa cells suggests that IRF-B is maximal after the peak of DNA synthesis and gradually decreases to a minimum at the $G_1$/S-phase boundary. Taken together, these results indicate a negative correlation between IRF-B activity in the nucleus and the onset of DNA replication.

Recently, a 28-kDa protein (Pur) from HeLa cell nuclei which recognizes the single-stranded purine-rich element located upstream of the c-myc gene near the center of a replication initiation zone has been reported (3). The derived consensus sequence, GGNNGAGGGAGARRR, has no homology to the SV40 IR domain, and therefore, it is unlikely that the Pur protein is identical to IRF-B. However, HeLa cell factors specifically binding to DNA sequences at the EBV latent origin of DNA replication have also been recently reported (34). Interestingly, the EBV sequence which partially competes for IRF-B binding to SV40 IR1 (Fig. 4) is a binding site for the reported HeLa cell factors.

If viral systems are a reflection of host DNA replication, one model for control of origin recognition may be constructed by opposing two specific single-stranded factors, whose binding and release may in turn be controlled by posttranslational modification. One pyrimidine-strand-specific factor (RPA) may function to constitutively destabilize the origin duplex, and the other sequence-specific factor may limit access to the region until the onset of S-phase, a limitation that may be bypassed in response to DNA damage.

## ACKNOWLEDGMENTS

## REFERENCES

1. Aladjem, M., Y. Koltin, and S. Lavi. 1987. Carcinogen mediated amplification of the CUP1 locus of Saccharomyces cerevisiae. Mol. Gen. Genet. 211:88–94.
2. Baer, R., A. T. Bankier, M. D. Biggin, P. L. Deininger, P. J. Farrell, T. J. Gibson, G. Hatful, G. S. Hudson, S. D. Satchwell, C. Seguin, P. S. Tuffnell, and B. G. Barrell. 1984. DNA sequence and expression of the B95-8 Epstein-Barr virus genome. Nature (London) 310:207–211.
3. Bergemann, A. D., and E. M. Johnson. 1992. The HeLa Pur factor binds single-stranded DNA at a specific element conserved in gene flanking regions and origins of DNA replication. Mol. Cell. Biol. 12:1257–1265.

4. **Berko-Flint, Y., S. Karby, D. Hassin, and S. Lavi.** 1990. Carcinogen-induced DNA amplification in vitro: overreplication of the simian virus 40 origin region in extracts from carcinogen-treated CO60 cells. Mol. Cell. Biol. **10:**75–83.

5. **Berko-Flint, Y., S. Karby, and S. Lavi.** 1989. Carcinogen-induced factors responsible for SV40 DNA replication and amplification in Chinese hamster cells, p. 133–141. *In* T. J. Kelly and B. Stillman (ed.), Cancer cells 6. Eukaryotic DNA replication. Cold Spring Harbor Laboratory, Cold Spring Harbor, N.Y.

6. **Boroweic, J. A., and J. Hurwitz.** 1988. Localized melting and structural changes in the SV40 origin of replication induced by T antigen. EMBO J. **7:**3149–3158.

7. **Bradford, M. M.** 1976. A rapid and sensitive method for the quantitation of microgram quantities of protein utilizing the principle of protein-dye binding. Anal. Biochem. **72:**248–254.

8. **Chang, L. M. S.** 1977. DNA polymerases from bakers' yeast. J. Biol. Chem. **252:**1873–1880.

8a.**Carmichael, E. P., and A. F. Wahl.** Unpublished observations.

9. **Chodosh, L. A., R. W. Carthew, and P. A. Sharp.** 1986. A single polypeptide possesses the binding and transcription activities of the adenovirus major late transcription factor. Mol. Cell. Biol. **6:**4723–4733.

10. **Cross, F., J. Roberts, and H. Weintraub.** 1989. Simple and complex cell cycles. Annu. Rev. Cell Biol. **5:**341–395.

11. **Crute, J. J., A. F. Wahl, and R. A. Bambara.** 1986. Purification and characterization of two new high molecular weight forms of DNA polymerase delta. Biochemistry **25:**26–36.

12. **Cunningham, T. P., and J. M. Pipas.** 1985. Simian agent 12 is a BK virus-like papovavirus which replicates in monkey cells. J. Virol. **54:**483–492.

13. **Dignam, J. D., R. M. Lebovitz, and R. Roeder.** 1983. Accurate transcription initiation by RNA polymerase II in a soluble extract from isolated mammalian nuclei. Nucleic Acids Res. **11:**1475–1489.

14. **Din, S., S. J. Brill, M. P. Fairman, and B. Stillman.** 1990. Cell-cycle-regulated phosphorylation of DNA replication factor A from human and yeast cells. Genes Dev. **4:**968–977.

15. **Ehrfeld, A., F. Planas-Bohne, and C. Lücke-Huhle.** 1986. Amplification of oncogenes and integrated SV40 sequences in mammalian cells by the decay of incorporated iodine-125. Radiat. Res. **108:**43–51.

16. **Fairman, M. P., and B. Stillman.** 1988. Cellular factors required for multiple stages of SV40 DNA replication *in vitro*. EMBO J. **7:**1211–1218.

17. **Fogel, M., and L. Sachs.** 1970. Induction of virus synthesis in polyoma transformed cells by ultraviolet light and mitomycin C. Virology **38:**174–177.

18. **Frisque, R. J., G. L. Bream, and M. T. Cannella.** 1984. Human polyomavirus JC virus genome. J. Virol. **51:**458–469.

19. **Hamatake, R. K., H. Hasegawa, A. B. Clark, K. Bebenek, T. A. Kunkel, and A. Sugino.** 1990. Purification and characterization of DNA polymerase II from the yeast *Saccharomyces cerevisiae*: identification of the catalytic core and a possible holoenzyme form of the enzyme. J. Biol. Chem. **265:**4072–4083.

20. **Kim, C., R. O. Snyder, and M. S. Wold.** 1992. Binding properties of replication protein A from human and yeast cells. Mol. Cell. Biol. **12:**3050–3059.

21. **Kleinberger, T., S. Etkin, and S. Lavi.** 1986. Carcinogen-mediated methotrexate resistance and dihydrofolate reductase amplification in Chinese hamster cells. Mol. Cell. Biol. **6:**1958–1964.

22. **Laemmli, U. K.** 1970. Cleavage of structural proteins during the assembly of the head of bacteriophage T4. Nature (London) **227:**680–685.

23. **Lambert, M. E., S. Gattoni-Celli, P. Kirschmeier, and I. B. Weinstein.** 1983. Benzo(a)pyrene induction of extrachromosomal viral DNA synthesis in rat cells transformed by polyoma virus. Carcinogenesis (London) **4:**587–593.

24. **Lambert, M. E., S. Pellegrini, S. Gattoni-Celli, and I. B. Weinstein.** 1986. Carcinogen-induced asynchronous replication of polyoma DNA is mediated by a *trans*-acting factor. Carcinogenesis (London) **7:**1011–1017.

25. **Lavi, S.** 1981. Carcinogen-mediated ampification of viral DNA sequences in simian virus 40-transformed Chinese hamster embryo cells. Proc. Natl. Acad. Sci. USA **78:**6144–6148.

26. **Lavi, S., T. Kleinberger, Y. Berko-Flint, and M. Blank.** 1987. Stable and transient coamplification of dhfr and SV40 in carcinogen treated cells, p. 117–125. *In* H. zur Hausen and J. R. Schlehofer (ed.), Accomplishments in oncology, vol. 2. J. B. Lippincott Co., Philadelphia.

27. **Lücke-Huhle, C., and P. Herrlich.** 1987. Alpha-radiation-induced amplification of integrated SV40 sequences is mediated by a *trans*-acting mechanism. Int. J. Cancer **39:**94–98.

28. **Lücke-Huhle, C., S. Mai, and P. Herrlich.** 1989. UV-induced early-domain binding factor as the limiting component of simian virus 40 DNA amplification in rodent cells. Mol. Cell. Biol. **9:**4812–4818.

29. **Lücke-Huhle, C., M. Pech, and P. Herrlich.** 1986. Selective gene amplification in mammalian cells after exposure to $^{60}$Co γ rays, $^{241}$Am α particles, or UV light. Radiat. Res. **106:**345–355.

30. **Marraccino, R. L., A. F. Wahl, P. C. Keng, E. M. Lord, and R. A. Bambara.** 1987. Cell cycle dependent activities of DNA polymerase alpha and delta in Chinese hamster ovary cells. Biochemistry **26:**7864–7870.

31. **Meistrich, M. L.** 1983. Experimental factors involved in separation by centrifugal elutriation, p. 33–61. *In* T. G. Pretlow II and T. P. Pretlow (ed.), Cell separation: methods and selected applications, vol. 2. Academic Press, New York.

32. **Morris, G. F., and M. B. Matthews.** 1989. Regulation of proliferating cell nuclear antigen during the cell cycle. J. Biol. Chem. **264:**13856–13864.

33. **Nomura, S., and M. Oishi.** 1984. UV irradiation induces an activity which stimulates simian virus 40 rescue upon cell fusion. Mol. Cell. Biol. **4:**1159–1162.

34. **Oh, S.-J., T. Chittenden, and A. J. Levine.** 1991. Identification of cellular factors that bind specifically to the Epstein-Barr virus origin of DNA replication. J. Virol. **65:**514–519.

35. **Parsons, R., M. E. Anderson, and P. Tegtmeyer.** 1990. Three domains in the simian virus 40 core origin orchestrate the binding, melting, and DNA helicase activities of T antigen. J. Virol. **64:**509–518.

36. **Riordan, J. R., K. Deuchars, N. Kartner, N. Alon, J. Trent, and V. Ling.** 1985. Amplification of P glycoprotein genes in multidrug resistant mammalian cell lines. Nature (London) **316:**817–819.

37. **Roberts, J. M., and G. D'Urso.** 1988. An origin unwinding activity regulates initiation of DNA replication during mammalian cell cycle. Science **241:**1486–1489.

38. **Ronai, Z. A., M. E. Lambert, M. D. Johnson, E. Okin, and I. B. Weinstein.** 1987. Induction of asynchronous replication of polyoma DNA by ultraviolet irradiation and the effect of various inhibitors. Cancer Res. **47:**4565–4570.

39. **Ronai, Z. A., and I. B. Weinstein.** 1988. Identification of a UV-induced *trans*-acting protein that stimulates polyomavirus DNA replication. J. Virol. **62:**1057–1060.

40. **Ronai, Z. A., and I. B. Weinstein.** 1990. Identification of ultraviolet-inducible proteins that bind to a TGACAACA sequence in the polyoma virus regulatory region. Cancer Res. **50:**5374–5381.

41. **Roninson, I. B., H. T. Abelson, D. E. Housman, N. Howell, and A. Varshavsky.** 1984. Amplification of specific DNA sequences correlates with multi-drug resistance in Chinese hamster cells. Nature (London) **309:**626–628.

42. **Schimke, R. T.** 1984. Gene amplification, drug resistance and cancer. Cancer Res. **44:**1735–1742.

43. **Schimke, R. T.** 1984. Gene amplification in cultured animal cells. Cell **37:**705–713.

44. **Schlehofer, J. R., M. Ehrbar, and H. Zur Hausen.** 1986. Vaccinia virus, herpes simplex virus and carcinogens induce DNA amplification in a human cell line and support replication of a helper virus dependent parvovirus. Virology **152:**110–117.

45. **Schorpp, M., W. Kugler, U. Wagner, and G. U. Ryffel.** 1988. Hepatocyte-specific promoter element HP1 of the *Xenopus* albumin gene interacts with transcriptional factors of mammalian hepatocytes. J. Mol. Biol. **202:**2787–2791.

46. **Stark, G. R., and G. M. Wahl.** 1984. Gene amplification. Annu. Rev. Biochem. **53:**447–491.

47. **Stow, N. D., and E. C. McMonagle.** 1983. Characterization of the TR$_S$/IR$_S$ origin of DNA replication of herpex simplex virus type 1. Virology **130:**427–438.

48. **Syväoja, J., S. Suomensaari, C. Nishida, J. S. Goldsmith, G. S. Chui, S. Jain, and S. Linn.** 1990. DNA polymerases alpha, delta, and epsilon: three distinct enzymes from HeLa cells. Proc. Natl. Acad. Sci. **87:**6664–6668.

49. **Thilly, W. G., T. S. Nowak, Jr., and G. N. Wogan.** 1974. Maintaining perpetual synchrony in HeLa S3 culture. Biotechnol. Bioeng. **16:**149–156.

50. **Tlsty, T. D., P. C. Brown, and R. T. Schimke.** 1984. UV irradiation facilitates methotrexate resistance and amplification of the dihydrofolate reductase gene in cultured 3T6 mouse cells. Mol. Cell. Biol. **4:**1050–1056.

51. **Tlsty, T. D., A. White, and J. Sanchez.** 1992. Suppression of gene amplification in human cell hybrids. Science **225:**1425–1427.

52. **Traut, W., and E. Fanning.** 1988. Sequence-specific interactions between a cellular DNA-binding protein and the simian virus 40 origin of DNA replication. Mol. Cell. Biol. **8:**903–911.

53. **Treger, J. M., J. Hauser, and K. Dixon.** 1988. Molecular analysis of enhanced replication of UV-damaged simian virus 40 DNA in UV-treated mammalian cells. Mol. Cell. Biol. **8:**2428–2434.

54. **Van der Lubbe, J. L. M., P. J. Abrahams, C. M. van Drunen, and A. J. van der Eb.** 1986. Enhanced induction of SV40 replication from transformed rat cells by fusion with UV-irradiated normal and repair-deficient human fibroblasts. Mutat. Res. **165:**47–56.

55. **Wahl, A. F., A. M. Geis, B. H. Spain, S. W. Wong, D. Korn, and T. S.-F. Wang.** 1988. Gene expression of human DNA polymerase alpha during cell proliferation and the cell cycle. Mol. Cell. Biol. **8:**5016–5025.

56. **Weinstein, I. B.** 1988. The origins of human cancer: molecular mechanisms of carcinogenesis and their implications for cancer prevention and treatment: twenty-seventh G.H.A. Clowes Memorial Award Lecture. Cancer Res. **48:**4135–4143.

57. **Wobbe, C. R., L. Weissbach, J. A. Borowiec, R. B. Dean, Y. Murakami, P. Bullock, and J. Hurwitz.** 1987. Replication of simian virus 40 origin-containing DNA *in vitro* with purified proteins. Proc. Natl. Acad. Sci. USA **84:**1834–1838.

58. **Wold, M. D., and T. Kelly.** 1988. Purification and characterization of replication protein A, a cellular protein required for *in vitro* replication of simian virus 40 DNA. Proc. Natl. Acad. Sci. USA **85:**2523–2527.

59. **Wold, M. S., J. J. Li, D. H. Weinberg, D. M. Virshup, J. L. Sherley, E. Verheyen, and T. J. Kelly.** 1988. Cellular proteins required for SV40 DNA replication *in vitro*, p. 133–141. *In* T. J. Kelly and B. Stillman (ed.), Cancer cells 6. Eukaryotic DNA replication. Cold Spring Harbor Laboratory, Cold Spring Harbor, N.Y.

60. **Yakobson, B., T. A. Hrynko, M. J. Peak, and E. Winocour.** 1989. Replication of adeno-associated virus in cells irradiated with UV light at 254 nm. J. Virol. **63:**1023–1030.